

# KeV scale new fermion from a hidden sector

We-Fu Chang<sup>1,\*</sup> and John N. Ng<sup>2,†</sup>

<sup>1</sup>*Department of Physics, National Tsing Hua University, No. 101,*

*Section 2, Kuang-Fu Road, Hsinchu, Taiwan 30013, R.O.C.*

<sup>2</sup>*TRIUMF, 4004 Wesbrook Mall, Vancouver, BC, V6T 2A3, Canada*

(Dated: December 15, 2024)

## Abstract

We studied a simple model of hidden sector consists of a Dirac fermion  $\chi$  and a spontaneously broken  $U(1)_s$  symmetry. The dark sector is connected to the Standard Model(SM) via three righthanded SM singlet neutrinos,  $N_R$ 's, and the kinetic mixing between  $U(1)_s$  and  $U(1)_Y$ . A mixing between the scalar  $\phi$  that breaks  $U(1)_s$  and the SM Higgs boson,  $H$ , is implemented via the term  $\phi^\dagger \phi H^\dagger H$  and this provides a third connection to the SM. Integrating out the  $N_R$  at a high scale not only gives the active neutrinos,  $\nu$ , masses but generates effective Dirac type of couplings between  $\nu$  and  $\chi$ . This changes the usual Type-I seesaw results for active neutrino masses and makes  $\chi$  behave like a sterile neutrino even though its origin is in the hidden sector.  $\chi$  is also split into a pair of Majorana fermions. The amount of splitting depends on the parameters. If the lighter of the pair has a mass around keV, its lifetime is longer than the age of the universe and it can be a warm dark matter candidate. Signatures of  $\chi$  in high precision Kurie plots of nuclei  $\beta$  decays and low energy neutrino nuclei coherent scatterings are discussed. The model also induces new invisible  $Z$  decay modes that can be searched for in future  $Z$  factories.

---

\*Electronic address: wfchang@phys.nthu.edu.tw

†Electronic address: misery@triumf.ca

## I. INTRODUCTION

Some time ago we investigated a very simple shadow  $U(1)_s$  sector which consists of a scalar  $\phi$  that spontaneously breaks the gauged abelian symmetry [1]. The resulting massive gauge boson  $X^\mu$  was allowed to kinetically mix with the hypercharge gauge boson  $B^\mu$  of the Standard Model (SM). The scalar  $\phi$  also couples to the SM Higgs field  $H$  via the term  $\phi^\dagger \phi H^\dagger H$ . In today's parlance, this will be the simplest two portal model respecting the SM gauge symmetry. The first portal is vector with the hypercharge as the mediator and the second is a scalar portal mediated by the Higgs boson.  $U(1)_s$  symmetry breaking scale characterized by  $v_s$  is taken to be above the electroweak breaking scale given by  $v = 247\text{GeV}$ . A scale-invariant version for the scalar sector was also constructed [2]. Moreover, the models did not yield a dark matter candidate. In this paper, we extend the model by adding a massive Dirac fermion  $\chi$  which is a SM singlet but is charged under the local  $U(1)_s$ . We also included at least two heavy righthanded SM singlet neutrinos,  $N_R$ , which are singlets under  $U(1)_s$ . Doing so enables us to use the type-I seesaw mechanism for active neutrinos masses. For clarity's sake, much of our discussion will be given for one  $N_R$  and extending to the realistic case of 3  $N_R$  is straight forward.  $N_R$  will also play the dual role of a fermion portal to the hidden sector. This constitutes a very simple complete minimal model with all three portals present.

Since the physics of the  $U(1)_s$  gauge boson and the scalar had been discussed thoroughly before, we shall concentrate here on the fermion  $\chi$ . In particular, we explore the parameter space which allows  $\chi$  to be a dark matter candidate. The minimal content of the hidden sector and using the conventional breaking of the  $U(1)_s$  does not leave us with a symmetry that can protect  $\chi$  from decaying and thus, in general, it cannot be stable. Without imposing an ad hoc symmetry, the only open option is to arrange  $\chi$  to be long-lived and plays the role of warm dark matter (WDM); similar to that of a sterile neutrino. Recently, WDM receives increasing attention due to its ability to address the small scale problem of the cold dark matter plus cosmological constant ( $\Lambda$ CDM) paradigm.  $\Lambda$ CDM have DM masses in the GeV to TeV range and predicts too many satellite galaxies in the Milky Way and cusped DM profiles which contradicts current observations. On the other hand, DM with masses in the keV range are capable of accommodating the number of observed satellites as well as cored profiles of dwarf galaxies which are believed to be DM-dominated.

The satellite problem arises because free relativistic particles do not cluster and they erase structures of scale smaller than the particle free-streaming length  $\ell_{\text{fs}}$  which is approximately the distance traveled before the particle becomes non-relativistic  $\sim c/3$ . For keV scale  $\ell_{\text{fs}} \sim 100\text{kpc}$ . On the contrary for CDM which is heavier and slower has  $\ell_{\text{fs}}$  million times smaller and leads to too many small scale structures [3]. While CDM is very successful in accounting for large scale structures and many other cosmological observations (see [4] for a review), it gives a steep cusp at the center for the galaxy density profile  $\rho \sim r^{-1}$  [5]. In contrast, WDM gives a finite constant density at the center  $\rho \sim \rho_0$  which is more in line with observations [6].

In addition, there are claims of the detection of a monochromatic line at 3.56 keV X-ray data towards the Andromeda and Perseus cluster [7] and [8]. This can be interpreted as the radiative decay of a fermion, usually taken to be sterile neutrino, into an active neutrino plus a photon. While this is suggestive, more mundane astrophysical explanation is also possible. Here we explore the possibility that monochromatic gamma can come from the radiative decay of  $\chi \rightarrow \nu + \gamma$  for a range of masses of interest in explaining the small scale structure conundrum. This motivates us to focus the  $\chi$  mass in the range of  $2 - 10\text{keV}$ . We shall see later that the astrophysical and cosmological properties of  $\chi$  we arrived at is almost indistinguishable from that of a sterile neutrino. A lucid review of sterile neutrino as warm dark matter can be found in [9]. We emphasize that  $\chi$  conceptually and physically is different from a sterile neutrino since it is not connected to active neutrino mass generation. As expected if  $\chi$  were to be a viable WDM candidate the parameter space of the model will be restricted.

The paper will be organized as follow. In Sec. 2, we will discuss in detail the model and how the role of high scale type-I seesaw plays in our study. This leads to the lifetime of  $\chi$  in Sec. 3. The implications of  $\chi$  for low energy precision neutrino physics are given in Sec.4. Effects on  $\beta$  decays of nuclei, neutrinoless double beta decays of nuclei and recently observed coherent low energy neutrino scattering producing  $\chi$  will be examined. This is followed by miscellaneous considerations of  $\chi$  at higher energies given in Sec.4. The main new result is the additional invisible decay of the SM  $Z$ . In Sec. 5 we discuss the cosmological requirements of  $\chi$  as the viable WDM and the limits this sets on the parameters of the model. Sec. 6 contains our conclusions.

Field	$\ell_L$	$H$	$N_R$	$\chi_L$	$\chi_R$	$\phi$
$SU(2)_L$	2	2	1	1	1	1
$U(1)_Y$	$-\frac{1}{2}$	$\frac{1}{2}$	0	0	0	0
$U(1)_s$	0	0	0	1	1	1

TABLE I:  $U(1)_s$  and SM quantum numbers for relevant fields.

## II. TYPE I SEESAW AND THE THREE PORTALS TO THE HIDDEN WORLD

In the usual notation, the gauge group of the model is  $SU(2)_L \times U(1)_Y \times U(1)_s$  where the color sector is omitted. We begin by discussing only one generation. The fields beyond the SM ones we use are SM singlet righthanded neutrino,  $N_R$ , the hidden Dirac fermion  $\chi$  which can be considered as a pair of different chiralities Weyl fermions  $\chi_{L,R}$ , a hidden sector scalar,  $\phi$  and the gauge field  $X_\mu$  of  $U(1)_s$ . The fields and their relevant quantum numbers are given in Table I.

The complete gauge invariant Lagrangian is given by

$$\begin{aligned}
\mathcal{L} &= \mathcal{L}_{\text{SMI}} + \mathcal{L}_{\text{sh}} + \mathcal{L}_{N\chi} \\
\mathcal{L}_{\text{SMI}} &= \mathcal{L}_{\text{SM}} + \overline{N_R} i \not{\partial} N_R - \left( y \bar{\ell}_L N_R \tilde{H} + \frac{1}{2} M_N \overline{N_R^c} N_R + h.c. \right) \\
\mathcal{L}_{\text{sh}} &= -\frac{1}{4} X^{\mu\nu} X_{\mu\nu} - \frac{\epsilon}{2} B^{\mu\nu} X_{\mu\nu} + \left| \left( \partial_\mu - i g_s X_\mu \right) \phi \right|^2 + \bar{\chi} (i \not{\partial} - g_s \not{X}) \chi - M_\chi \bar{\chi} \chi - V(\phi, H) \\
\mathcal{L}_{N\chi} &= -f_L \overline{\chi_L} N_R \phi - f_R \overline{\chi_R^c} N_R \phi^* + h.c. \\
V(H, \phi) &= -\mu_s^2 \phi^* \phi + \lambda_s (\phi^* \phi)^2 + \kappa (H^\dagger H) (\phi^* \phi) - \mu^2 H^\dagger H + \lambda (H^\dagger H)^2
\end{aligned} \tag{1}$$

where  $\ell_L, H$  are the SM lepton doublet and the Higgs field respectively with  $\tilde{H} = i\sigma_2 H$ .  $B_{\mu\nu}$  is the field strength tensor of  $U(1)_Y$  and  $g_s$  is the gauge coupling of  $U(1)_s$ . We have arbitrarily chosen  $\chi, \phi$  to have unit shadow charge with convention given in Eq.(1). It is interesting to note that a conventional lepton number of one unit can be assigned to  $\chi$  and 0 for  $\phi$ . But it is not necessary since the Majorana mass term for  $N_R$  breaks that explicitly by two units. The portal terms are  $\epsilon$  in  $\mathcal{L}_{\text{sh}}, \mathcal{L}_{N\chi}$  and the  $\kappa$  term in  $V(H, \phi)$ .

Next, we implement the type-I seesaw mechanism. This means that we shall assume that  $M_N$  is much heavier than any other masses and integrate out  $N_R$ . The easiest way to do

this is diagrammatical. This generates some dimension five terms below the scale  $M_N$  as depicted in the Feynman diagrams given in Fig.(1). The effective theory below the seesaw

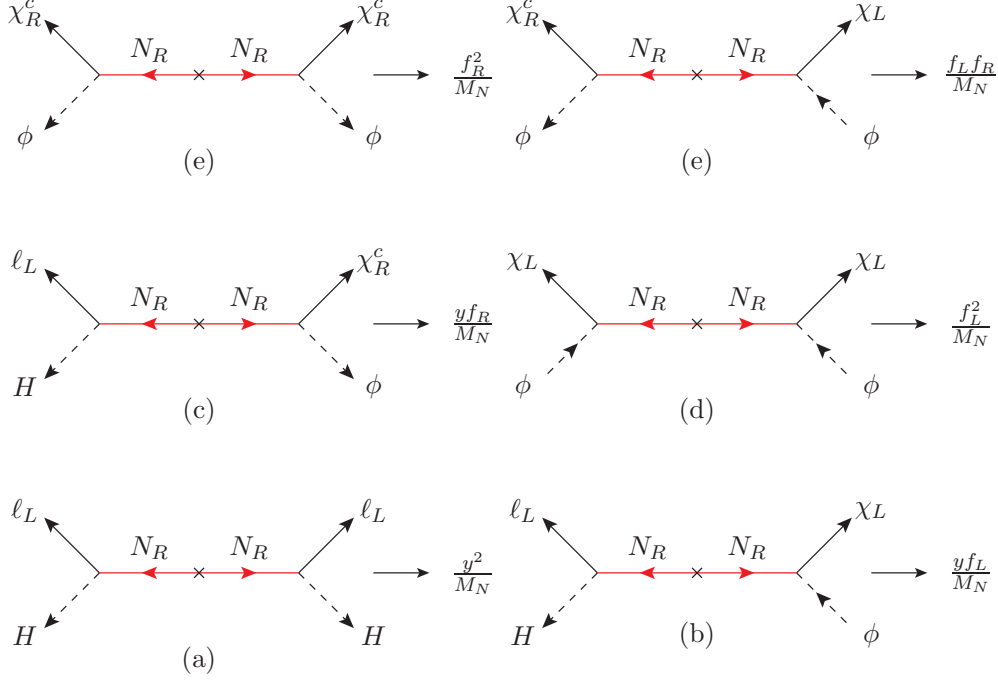


FIG. 1: Integrating out the heavy  $N_R$

scale will then consists of  $\mathcal{L}_{\text{SM}} + \mathcal{L}_{sh}$  and  $\mathcal{L}_5$  where

$$\begin{aligned}
 -M_N \mathcal{L}_5 = & y^2 \overline{\ell_L^c} \ell_L H H + y f_L \overline{\chi_L^c} \phi^* \ell_L H + y f_R \overline{\chi_R} \ell_L \phi H \\
 & + f_L^2 \overline{\chi_L} \chi_L \phi^* \phi^* + f_R^2 \overline{\chi_R} \chi_R \phi^* \phi^* + f_L f_R \overline{\chi_L} \chi_R \phi \phi^* + h.c.
 \end{aligned} \tag{2}$$

After spontaneous symmetry breaking (SSB) with  $\langle H \rangle = v/\sqrt{2}$ , one gets the familiar Weinberg operator [10] for active neutrinos mass  $\sim \frac{y^2 v^2}{2M_N}$ , see Fig. (1a). In addition, we also have SSB for  $U(1)_s$  via  $\langle \phi \rangle = v_s/\sqrt{2}$ . This induces a mass mixing with the hidden fermion given by  $\sim \frac{y f_{L/R} v v_s}{2M_N}$  (Fig.(1b)). Repeating this for all the diagrams of Fig.(1) yields for one SM generation a  $3 \times 3$  effective neutrino mass matrix  $M_\nu$ . In the weak basis  $\{\nu, \chi_L, \chi_R^c\}$  it is given by

$$M_\nu \sim \begin{pmatrix} y^2 \frac{v^2}{M_N} & y f_L \frac{v v_s}{2M_N} & y f_R \frac{v v_s}{2M_N} \\ y f_L \frac{v v_s}{2M_N} & f_L^2 \frac{v_s^2}{M_N} & \frac{1}{2}(M_\chi + f_L f_R \frac{v_s^2}{M_N}) \\ y f_R \frac{v v_s}{2M_N} & \frac{1}{2}(M_\chi + f_L f_R \frac{v_s^2}{M_N}) & f_R^2 \frac{v_s^2}{M_N} \end{pmatrix}. \tag{3}$$

We reiterate that  $M_\nu$  is a consequence of generalizing the high scale type-I seesaw mechanism to include the fermion portal Lagrangian with SSB taken afterwards. Thus, the hierarchy of

scale we are interested in is  $M_N \gg v_s \gtrsim v$ . It is easy to see that with this hierarchy entries of the active neutrino masses, i.e. the upper most left corner of Eq.(3) is in the sub-eV range for  $\frac{y^2}{M_N} \simeq 10^{-14}(\text{GeV})^{-1}$ . We shall use the benchmark point of  $M_N = 10^{10} \text{ GeV}$ ,  $y = 10^{-2}$  and  $v_s = 1 \text{ TeV}$ . Thus,  $\frac{v_s^2}{M_N} \simeq 100 \text{ keV}$  and  $\frac{vv_s}{M_N} \simeq 10 \text{ keV}$ . We also work in the perturbative regime and hence take  $f_{L/R} \lesssim 1$ . Specifically if we take  $M_\chi \sim 10 \text{ keV}$  and  $f_L = f_R = 0.1$ , we have

$$M_\nu \simeq \begin{pmatrix} y^2 \frac{v^2}{M_N} & y f_L \frac{vv_s}{2M_N} & y f_R \frac{vv_s}{2M_N} \\ y f_L \frac{vv_s}{2M_N} & f_L^2 \frac{v_s^2}{M_N} & \frac{1}{2} M_\chi \\ y f_R \frac{vv_s}{2M_N} & \frac{1}{2} M_\chi & f_R^2 \frac{v_s^2}{M_N} \end{pmatrix}. \quad (4)$$

It is easy to see that the splitting of  $\chi_L$  and  $\chi_R$  arises from the  $f_{L,R}^2$  terms. For  $f_{L/R} \sim 0.1$  this is  $\mathcal{O}(1 \text{ keV})$ . Thus,  $\chi$  will remain essentially a Dirac fermion for this range of parameters. As a reminder,  $M_\chi$  is not the physical mass. Even smaller splitting can be obtained by taking  $f < 1$ . We note that the physical states are actually two Majorana neutrinos  $\chi_1, \chi_2$  with masses so close to each other that most experiments cannot resolve them.

For larger splitting we have to explore a different parameter region. If we take  $f_L = f_R \sim 1$ , then  $\frac{f^2 v_s^2}{M_N} \sim 100 \text{ keV}$ . For  $M_\chi \sim 80 \text{ keV}$ , the original Dirac  $\chi$  will now split into two Majorana fermions one with mass  $\sim 100 \text{ keV}$  and the other  $\sim 10 \text{ keV}$ . One more example is to take  $M_N = 10^8 \text{ GeV}$  with  $y = 10^{-3}$  so that the active neutrino masses will be in the sub-eV range via Type-I seesaw. With  $f \simeq 0.3$ ,  $M_\chi \sim \text{MeV}$  it will yield a mass at around  $10 \text{ keV}$  and the other at about  $\text{MeV}$ . From this exercise, it is clear to see that the mass splitting becomes more substantial if the lepton number violation scale,  $M_N$ , is lower and/or  $v_s, M_\chi$  are raised. Moreover, only the lighter one can be the WDM to solve the small scale problem of CDM. Nevertheless, the more massive partner can have interesting phenomenology as we shall see later.

To make the physics more transparent how the above considerations can alter the type-I seesaw mechanism for active neutrino mass generation and the value of the eventual physical mass of  $\chi$ , we again setting  $f_L = f_R = f$ ,  $y = 1$ ,  $M_N = 10^{14} \text{ GeV}$ , and ignore the splitting discussed above. The mixing of active  $\nu$  is with a Dirac shadow fermion  $\chi$ . The simplified neutral fermion mass matrix  $M_\nu^s$  becomes

$$M_\nu^s \simeq \begin{pmatrix} \frac{v^2}{M_N} & \frac{f v v_s}{2M_N} \\ \frac{f v v_s}{2M_N} & M_\chi \end{pmatrix}. \quad (5)$$

The eigenvalues are

$$M_0^\pm = \frac{M_\chi}{2} \left[ (1+a) \pm \sqrt{(1-a)^2 + 4b^2} \right] \quad (6)$$

where  $a = \frac{v^2}{M_\chi M_N}$  and  $b = \frac{f v v_s}{2 M_\chi M_N}$  and  $a, b \ll 1$  for  $M_\chi > 100\text{eV}$ . Thus,

$$M_0^+ \simeq M_\chi \left[ 1 + \left( \frac{f v v_s}{2 M_\chi M_N} \right)^2 \right] \quad (7)$$

$$M_0^- \simeq \frac{v^2}{M_N} \left[ 1 - \left( \frac{f^2 v_s^2}{4 M_\chi M_N} \right) \right]. \quad (8)$$

The physical mass of  $\chi$  is pushed up but not changed by much. On the other hand, the physical mass of the active neutrino is pushed down compared from the type-I seesaw value.

It is instructive to look at some typical numbers.  $M_\chi$  is a free parameter. If we take  $v_s = 1\text{TeV}$ ,  $M_N = 10^{14}\text{GeV}$  (here we set  $y = 1$ ) the correction to  $M_\chi = 1\text{keV}$  is negligibly small. In contrast, the correction to the seesaw active neutrino mass is  $\sim f^2\%$  (see. Eq.(8)) which can be substantial if  $f > 1$ . Furthermore, the correction is more significant for smaller values of  $M_\chi$ .

The mixing angle is given by

$$\theta \simeq \frac{y f v v_s}{2 M_\chi M_N}. \quad (9)$$

As expected, the heavier  $\chi$  is, the smaller is the mixing with the SM active neutrino. Furthermore, its effect on the active neutrino mass is also less. In many aspects, it behaves very much like a sterile neutrino although it originates from a hidden sector.

It is important to note  $\mathcal{L}_5$  also gives rise to dimension-4 operators when only one of the scalar fields pick up a VEV. An example will be  $\frac{v_s}{M_N} f_R \overline{\chi_R} \ell_L H$ , which is not present in the original Lagrangian. This can lead to invisible decay modes for the Higgs boson if  $\chi$  is sufficiently light. However, the effective coupling is expected to be  $\mathcal{O}(10^{-10})$ , and the decay cannot be detected in the near future. The rest of similar terms can be read off from Eq.(2) and they all have seesaw suppressed couplings.

Generalizing to the 3 active neutrino case is straightforward. For simplicity we set  $f_L = f_R = f$  and the neutral fermion mass matrix is now  $5 \times 5$  matrix since  $\chi$  is now split into two Majorana fermions denoted by  $\chi_{1,2}$ . In the weak interaction basis,  $\nu_\alpha, \alpha = e, \mu, \tau, \chi_L, \chi_R^c$

and ignore the seesaw suppressed Majorana masses to  $\chi_{R,L}$ , this is given by

$$\mathcal{M}_\nu \simeq \begin{pmatrix} \frac{y_{ee}v^2}{M_N} & \frac{y_{e\mu}v^2}{M_N} & \frac{y_{e\tau}v^2}{M_N} & \frac{y_{ef}vv_s}{M_N} & \frac{y_{ef}vv_s}{M_N} \\ \frac{y_{e\mu}v^2}{M_N} & \frac{y_{\mu\mu}v^2}{M_N} & \frac{y_{\mu\tau}v^2}{M_N} & \frac{y_{\mu f}vv_s}{M_N} & \frac{y_{\mu f}vv_s}{M_N} \\ \frac{y_{e\tau}v^2}{M_N} & \frac{y_{\mu\tau}v^2}{M_N} & \frac{y_{\tau\tau}v^2}{M_N} & \frac{y_{\tau f}vv_s}{M_N} & \frac{y_{\tau f}vv_s}{M_N} \\ \frac{y_{ef}vv_s}{M_N} & \frac{y_{\mu f}vv_s}{M_N} & \frac{y_{\tau f}vv_s}{M_N} & 0 & \frac{1}{2}M_\chi \\ \frac{y_{ef}vv_s}{M_N} & \frac{y_{\mu f}vv_s}{M_N} & \frac{y_{\tau f}vv_s}{M_N} & \frac{1}{2}M_\chi & 0 \end{pmatrix} \quad (10)$$

where we have restored the various Yukawa couplings of active neutrino  $N_R$  couplings and  $y_{\alpha\alpha'} = \frac{1}{2}y_\alpha y_{\alpha'}$ ,  $y_{\alpha f} = \frac{1}{2}y_\alpha f$ . The mass basis  $\nu_i, i = 1 \cdots 5$  is related to the weak basis by a unitary transformation :  $\nu_\alpha = \sum_i U_{\alpha i} \nu_i$ . This diagonalizes Eq.(10), i.e.  $M_\nu^{diag} = U^\dagger \mathcal{M}_\nu U$ . The weak charged current in the mass basis can be obtained from

$$\frac{ig}{\sqrt{2}} \sum_{\alpha=e,\mu,\tau} \sum_{i=1}^5 U_{\alpha i} \bar{e}_\alpha \gamma_{\mu L} \nu_i W^{\mu,-} + h.c. \quad (11)$$

Without going into the detail numerical analysis of neutrino oscillation data, one can expect that  $U_{\alpha 4,5}$  to be approximately given by Eq.(9). Similarly, with the help of unitarity of  $U$ , the neutral current involving neutrinos in the mass basis can be deduced to be

$$\frac{ig}{2 \cos \theta_w} \left[ \sum_{i=1}^5 \bar{\nu}_i \gamma_{\mu L} \nu_i - \left( \sum_{i,j=1}^5 (U^\dagger)_{j\chi L} U_{\chi L i} \bar{\nu}_j \gamma_{\mu L} \nu_i + \sum_{i,j=1}^5 (U^\dagger)_{j\chi R} U_{\chi R i} \bar{\nu}_j \gamma_{\mu L} \nu_i \right) \right] Z^\mu. \quad (12)$$

For  $i, j \neq 4, 5$  there is a small off-diagonal coupling that can be neglected. For the diagonal term the coupling strength is essentially that of the SM since the second term is negligible.

It is clear that since  $\chi$  can mix with the active neutrino with a small mixing angle, it behaves very much like a sterile neutrino. It has similar charged and neutral currents interactions as a sterile neutrino would through mixing. However, its origin is very different from the sterile neutrino commonly studied. There are numerous models for sterile neutrinos. It is useful to compare our case with a complete model of sterile neutrino to bring out the differences. The well-known example is the Neutrino Minimal Standard Model ( $\nu$ MSM) [11] which is a low scale seesaw model, i.e., the lepton number breaking scale is below the Fermi scale. There are three sterile neutrinos corresponding to the three  $N_R$ 's, two of which are in the GeV range and the third is the keV range. The last one is identified as WDM. This is the only state in this mass range. On the other hand,  $\chi$  consists of two nearly degenerate states. If the splitting is  $> 100\text{keV}$ , optimistically, this can be seen in near future experiments (see Sec.5) and thus offers a distinction from the sterile neutrino scenario. Otherwise,  $\chi$  will be



a pseudo-Dirac fermion. In this case, it will be more difficult to tell two scenarios apart. It may be necessary to examine other signals.

### III. STABILITY OF THE SHADOW FERMION

It is clear from the previous discussions that none of the hidden sector fields can be stable after SSB. For  $\chi$  to play the role of WDM we assume that is the lightest of the hidden particles. Denoting the mass eigenstates by  $\chi_{\pm}$  and requiring that they have masses in the  $\mathcal{O}(10\text{keV})$  range the only available decays are  $\chi_{\pm} \rightarrow 3\nu$  and  $\chi_{\pm} \rightarrow \nu\gamma$ . The width of the invisible decays is given by

$$\Gamma(\chi_{\pm} \rightarrow 3\nu) = \frac{G_F^2 M_{\chi}^5}{96\pi^3} \sum_{i=1}^3 |U_{\chi i}|^2. \quad (13)$$

as they are Majorana states.

The radiative decay is a 1-loop effect. Unlike most loop effects the model dependence can be reduced to only the mixing angle by calculating the width in the U-gauge. The width is given by<sup>1</sup>

$$\Gamma(\chi_{\pm} \rightarrow \gamma\nu) = \frac{9\alpha G_F^2}{256\pi^4} M_{\chi}^5 \sum_{\alpha=e,\mu,\tau} \sum_{i=1,2,3} |U_{4\alpha}|^2 |U_{\alpha i}|^2 \quad (14)$$

The invisible decays will be faster than the radiative mode. For  $M_{\chi} = 10\text{keV}$  and a lifetime longer than that of the universe will give the constraint

$$\sum_{i=1}^3 |U_{\chi i}|^2 < 1.8 \times 10^{-2}. \quad (15)$$

This is to be compared with the expectation of  $\sim 10^{-4}$  given by Eq.(9) for  $v_s = 1\text{TeV}$ . This validates  $\chi_{\pm}$  as WDM candidates. This decay will give a monochromatic X-ray line for each of the  $\chi$ 's if the splitting is larger than the experimental resolution but still small enough to be in the  $< 10\text{keV}$  range.

Next, we consider the scenario that  $\chi$  splits into two Majorana neutrinos one with mass  $10\text{keV}$  and the other  $100\text{keV}$ . The lifetime of the heavier one is estimated to be  $\sim 3.3 \times$

---

<sup>1</sup> This is in agreement with the result of [12]. The calculation there was done in the Feynman gauge and is valid for the sterile neutrino in Type-I seesaw model. Our U-gauge calculation shows that this result holds for any SM singlet fermion that mixes with the active neutrinos and independent of how the individual masses are obtained.

$10^5$  years with the same mixing as in Eq.(15). This will not affect the cosmic microwave background measurements and thus can also be a viable cosmological scenario. It may have later time cosmological implications which are beyond the scope of this investigation.

#### IV. IMPLICATIONS FOR LOW ENERGY NEUTRINO PHYSICS

##### A. $\beta$ decay spectrum

It is well known that a detailed study of the  $\beta$  decay spectrum of nuclei can reveal the existence of one or more heavy neutrinos. This has been studied in the context of Kaluza-Klein extra dimensional models [13] where there can be many such neutrinos. More recently, a detailed study has been conducted for tritium decays [14]. The KATRIN experiment [15] can also be used to look for neutral leptons of mass lower than 18 keV.

For a nuclear  $\beta$  decay with its mass  $\gg Q, E_e, m_{\nu_\alpha}$ , the differential decay rate as a function of electron energy  $E_e$  is given by the leading approximation

$$\begin{aligned} \frac{dR}{dE_e} = & K_\beta E_e (Q + m_e - E_e) (E_e^2 - m_e^2)^{\frac{1}{2}} \\ & \left\{ |U_{e5}|^2 [(Q + m_e - E_e)^2 - M_2^2]^{\frac{1}{2}} + |U_{e4}|^2 [(Q + m_e - E_e)^2 - M_1^2]^{\frac{1}{2}} \right. \\ & \left. + \sum_{i=1}^3 |U_{ei}|^2 [(Q + m_e - E_e)^2 - m_i^2]^{\frac{1}{2}} \right\}. \end{aligned} \quad (16)$$

where  $K_\beta$  includes the nuclear matrix element, the Fermi function, and  $G_F$ . And  $Q$  is the  $Q$ -value of 18.59 keV for tritium. We have also separated the heavy Majorana fermions  $\chi_2, \chi_1$  with masses  $M_2, M_1$  from the physical active neutrinos given in the last term. The spectrum consists of three branches if the energy resolution is smaller than  $M_2 - M_1$ . The first one will cut off at

$$E_e = Q + m_e - M_2 \quad (17)$$

and give a kink at that point. The second kink appears at

$$E_e = Q + m_e - M_1. \quad (18)$$

To illustrate, we display the differential decay rates in Fig. Fig.2(a) with a unrealistic sizable mixing  $|U_{e4,5}| = 0.4$  for two representative sets of  $M_1, M_2$ .

In Fig.2(b), we display the ratio of the same Kurie plot to that of the SM derivation from unit for two representative sets of  $M_1, M_2$ .

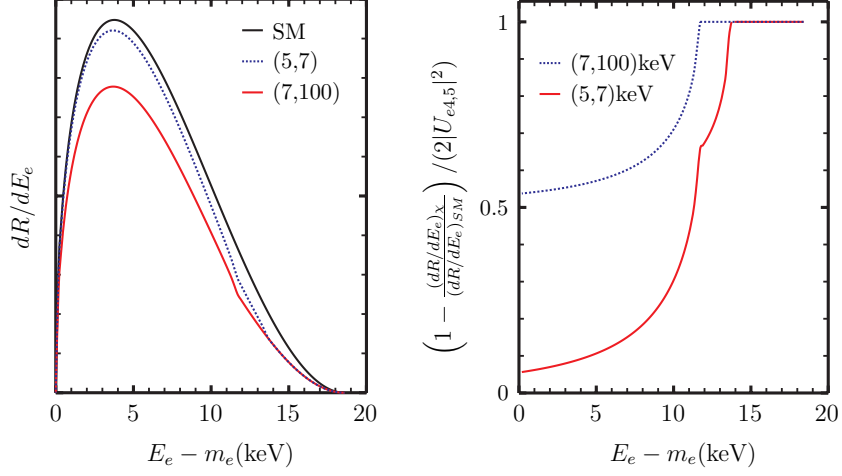


FIG. 2: (a)  $dR/dE_l$ , in arbitrary unit, vs  $E_l - m_e$  (in keV). Black line denotes the SM curve. The dotted blue line is for  $(M_1, M_2) = (7, 5)$  keV, and the red one is for  $(M_1, M_2) = (7, 100)$  keV. The mixings are  $U_{e4} = U_{e5} = 0.4$ . (b)  $1 - \frac{(dR/dE_l)_X}{(dR/dE_l)_{SM}}$  in unit of  $2|U_{e4,5}|^2$ .  $(M_1, M_2) = (7, 5)$  and  $(7, 100)$  keV.

If the energy resolution is not sufficient to resolve the two masses, then one smeared kink will appear in the spectrum before it cuts off at  $E_e \simeq 18.59$  keV and gives the usual result of

$$m_{\nu_e} = \sqrt{\sum_{i=1}^3 |U_{ei}|^2 m_i^2}. \quad (19)$$

To be able to observe kink-like structure in the spectrum the energy resolution will have to be approximately 300 eV in this energy range, and a dedicate experiment is being proposed [16]. A limit on the mixing of  $|U_{e4,5}|^2 \lesssim 10^{-7}$  can be set if no kinks were found.

### B. $0\nu\beta\beta$ decays of nuclei

For Majorana neutral fermions of mass less than 100 keV and mix with the SM active neutrinos, the usual neutrino exchange mechanism for  $0\nu\beta\beta$  decays of nuclei is still applicable. The effective Majorana mass for  $\nu_e$  denoted by  $m_{ee}$  is given by

$$m_{ee} = \left| U_{e1}^2 m_1 + U_{e2}^2 e^{2i\alpha_2} m_2 + U_{e3}^2 e^{2i\alpha_3} m_3 + U_{e4}^2 e^{2i\alpha_4} M_1 + U_{e5}^2 e^{2i\alpha_5} M_2 \right|, \quad (20)$$

where  $\alpha_j, j = 2 \dots 5$  are the Majorana phases. There are now four such phases in addition to the Dirac phases in  $U_{ei}$  which now total 3. It is instructive to compare the contributions

of the SM active neutrinos versus the  $\chi$ 's. Without going into the details, one expects the active neutrinos to contribute  $10^{-2} - 10^{-3}$  eV to  $m_{ee}$ . Using Eq.(9) as a guide, they contribute  $10^{-4} - 10^{-2}$  eV, depending on the Yukawa, for  $M_{1,2} \sim 10\text{keV}$ . Hence, the mixing of  $\chi$  with the SM neutrinos will significantly change the expectations of  $0\nu\beta\beta$  decays.

### C. Coherent low energy neutrino production of $\chi$

We have argued that  $\chi$  can be a warm dark matter candidate if its mass is in the keV range. It is a prime candidate for production in low energy coherent neutrino-nucleus scattering ( $\text{CE}\nu\text{NS}$ ) which has been observed recently in the COHERENT experiment [17] at a spallation neutron source. Such experiments can also be carried out at high powered reactors. The principal experimental challenge is to detect very low nuclear recoils. Cryogenic bolometers harbor the promise to detect sub 100 eV recoils [18].

The most important physics requirement for  $\text{CE}\nu\text{NS}$  is a small momentum transfer to the nucleus. This has to be smaller than the inverse radius of the nucleus in order to maintain coherence. The scattering process must also not alter the quantum state of the nucleus. Nuclear excitations must not be triggered otherwise it will break the coherence of nucleons that are scattered. We studied the process

$$\nu + \mathcal{N} \rightarrow \chi + \mathcal{N} \quad (21)$$

where  $\mathcal{N}$  denotes the nucleus. We are interested in how Eq.(21) can be used to limit the parameter space of the model.

The two main fundamental processes are due to  $Z$  and  $H$  exchanges as shown in Fig.(3). The one-photon exchange process is very small in our model and can be ignored. The two main processes have the same kinematics but give different differential cross sections  $\frac{d\sigma}{dT}$  where  $T$  is the recoil energy of the nucleus. The  $Z$  exchange process is similar to the SM coherent scattering and thus is suppressed by the  $\nu - \chi$  mixing. It is well known that it is sensitive to the weak charge of the nucleus  $Q_w = N - Z(1 - 4\sin^2\theta_W)$  and  $N(Z)$  represents the number of neutrons(protons)in the nucleus. Due to the accidental cancelation of the proton weak charge this cross section is expected to scale as  $N^2$ . Moreover, we can view (a) as an additional branch to the SM process much the same way it adds to the  $\beta$  decay spectrum studied earlier.

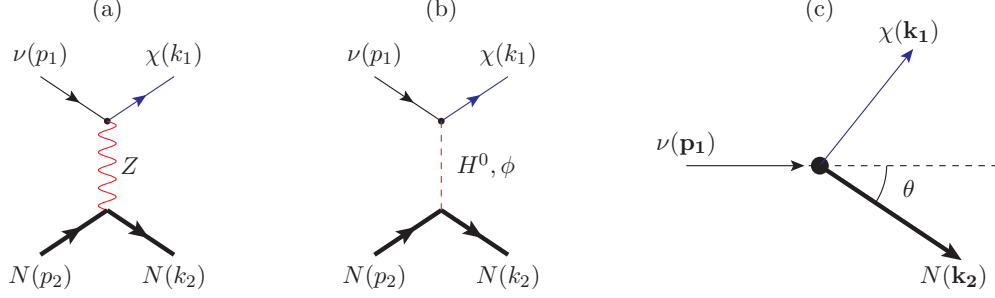


FIG. 3: Coherent  $\nu$  production of  $\chi$  via (a)  $Z$  boson, (b) Higgs boson exchange and The fixed target kinematics is depicted in (c)

On the other hand, (b) has no SM equivalence since it requires the existence of a righthanded singlet fermion such as sterile neutrino. Here  $\chi$  plays that role although it is not a sterile neutrino per se. Furthermore, (b) is sensitive to Higgs nucleon coupling,  $g_{Hnn} = \frac{gM_N}{2M_W}\eta$  where  $\eta \simeq 0.3$  [19] and  $M_N$  is the nucleon mass. This coupling is both experimentally and theoretically interesting. Neglecting the small neutron-proton mass difference and use  $M_N \rightarrow M$  where  $M$  is the mass of the nucleus. Roughly speaking we can take  $M \approx AM_N, A = N + Z$ .

The two important kinematic quantities are the scattering angle  $\theta$  (see Fig.(3 c)), and the recoil energy  $T$ . In terms of  $T$ , the scattering angle is

$$\cos \theta = \frac{E_\nu T + MT + \frac{1}{2}m_\chi^2}{E_\nu \sqrt{T^2 + 2MT}}. \quad (22)$$

where  $E_\nu$  is the incoming neutrino energy, and  $M$  is From this, we obtain the maximum  $T_+$  and a minimum  $T_-$  allowed recoil energies

$$T_{\pm} = \frac{ME_\nu^2 - \frac{1}{2}m_\chi^2(M + E_\nu) \pm E_\nu [M^2E_\nu^2 - m_\chi^2M(M + E_\nu) + \frac{1}{4}m_\chi^4]^{\frac{1}{2}}}{M(M + 2E_\nu)}. \quad (23)$$

We recover the SM values by taking  $m_\chi = 0$ . Hence  $T_+^{\text{SM}} = \frac{2E_\nu^2}{(M+2E_\nu)}$  and  $T_-^{\text{SM}} = 0$ . The differential cross section can be written as

$$\frac{d\sigma^a}{dT} = \frac{1}{32\pi} \frac{1}{ME_\nu^2} \left[ \frac{1}{2} \sum_{\text{spins}} |\mathcal{M}|^2 \right] \quad (24)$$

where  $\mathcal{M}$  is the invariant amplitude. The cross sections are the same for  $\bar{\nu}$ . For the  $Z$  exchange process we have

$$\frac{d\sigma^{(Z)}}{dT} = \frac{G_F^2 Q_W^2 |U_{\ell 4}|^2}{4\pi} M \left[ 1 - \frac{MT}{2E_\nu^2} - \frac{T}{E_\nu} + \frac{T^2}{2E_\nu^2} - \frac{m_\chi^2}{4E_\nu^2} \left( \frac{2E_\nu}{M} - \frac{T}{M} + 1 \right) \right] F_Z^2(q^2) \quad (25)$$

where  $F$  is the nuclear form factor for the specific nucleus used in the detector, and  $q^2 = -2MT$  is the momentum transfer squared. For  $m_\chi = 0$ , it reduces to the well-known SM result [20]. Here  $\ell$  is the flavor of the incoming neutrino. For reactor neutrinos  $\ell = e$  and for spallation neutron source  $\ell = \mu, e$ . Similarly, the cross section due to scalar exchanges is

$$\frac{d\sigma^{(H)}}{dT} = \frac{y_\chi^2 g_{HNN}^2}{4\pi} M \cos^2 \alpha \left( \frac{1}{M_H^2} + \frac{v \tan \alpha}{v_s M_\phi^2} \right)^2 \left( 1 + \frac{T}{2M} \right) \left( \frac{MT}{E_\nu^2} + \frac{m_\chi^2}{2E_\nu^2} \right) F_H^2(q^2) \quad (26)$$

where  $y_\chi$  parameterizes the new dimension-4  $H - \nu - \chi$  coupling (see Fig.(1)) and  $\alpha$  is the mixing angle of Higgs and  $\phi$ . We have included  $\phi$  exchange although it is suppressed by the ratio of vev's and the mixing  $\alpha$  as seen above. In the range of  $M_\phi \sim \mathcal{O}(\text{GeV})$  this can be comparable to the Higgs exchange effect. The Higgs coupling to nucleus  $g_{HNN}$  is an unknown quantity. However, we shall take it to be  $g_{nn}$  with the substitution  $m_n \rightarrow M$ . Admittedly this is a gross attempt to capture the nucleon coherent effect. Furthermore, in general the form factor  $F_H$  is different from  $F_Z$  in Eq.(25).

For the signal, we have to integrate over the appropriate neutrino spectrum. In general, the differential number of events per unit time is given by

$$\frac{dN^{(a)}}{dT} = n_i \int_{E_{\nu\min}}^{E_{\nu\max}} dE_\nu \phi(E_\nu) \frac{d\sigma^{(a)}}{dT}(T, E_\nu) \quad (27)$$

where  $n_i$  is the number of target nuclei in the detector,  $\phi(E_\nu)$  is the flux of the incoming neutrinos,  $E_{\nu\max}$  is the maximum source neutrino energy,  $E_{\nu\min}$  is the minimum required neutrino energy to induce the given recoil  $T$  given by

$$E_{\nu\min} = \frac{MT + m_\chi^2/2}{\sqrt{2MT + T^2} - T} \simeq \sqrt{MT/2}, \quad (28)$$

and  $a = \text{SM}, Z, H$  and can be read off from Eqs.(25,26). For a target with atomic number  $A$ , the minimal neutrino energy is  $\sim 7 \times \sqrt{A/100} \text{ MeV}$  to generate a recoil energy of  $T = 1 \text{ keV}$ . For a neutrino source with energy  $E_\nu$  and  $m_\chi, E_\nu \ll M$ , the maximal recoil energy is about  $T_+ \sim 20 \times (E_\nu/\text{MeV})^2 \times (100/A) \text{ eV}$ . Therefor, the maximal recoil energy in the  $\nu + N \rightarrow \chi + N$  process is about  $\mathcal{O}(1)$  and  $\mathcal{O}(40) \text{ keV}$  for neutrinos from a nuclear power plant and a spallation neutron source, respectively.

The COHERENT experiment [17] utilizes neutrinos from a spallation source. There are three flavors of incoming neutrinos from  $\pi^+$  decays almost at rest into  $\mu^+ + \nu_\mu$  and the muon subsequently decays into  $e^+ \bar{\nu}_\mu \nu_e$ . The  $\nu_\mu$  from the first decay gives a monochromatic flux.

The muon decays are usually taken to be almost at rest. However, it is easy to take into account the energy of the muon which is given by  $E_\mu = \frac{m_\pi^2 + m_\mu^2}{2m_\pi} = 109.78\text{MeV}$ . The fluxes are calculated to be

$$\phi_{\nu_\mu}(E_\nu) = \phi_0 \delta\left(E_\nu - \frac{m_\pi^2 - m_\mu^2}{2m_\pi}\right), \quad (29a)$$

$$\phi_{\nu_e}(E_\nu) = \phi_0 \frac{192}{m_\mu} \left(\frac{E_\nu E_\mu}{m_\mu^2}\right)^2 \left[\frac{m_\mu}{2E_\mu} - \frac{E_\nu}{m_\mu} \left(1 + \frac{\mathbf{p}_\mu^2}{3E_\mu^2}\right)\right], \quad (29b)$$

$$\phi_{\bar{\nu}_\mu}(E_\nu) = \phi_0 \frac{64}{m_\mu} \left(\frac{E_\nu^2}{m_\mu^2}\right) \left[\frac{3}{4} - \frac{E_\nu E_\mu}{m_\mu^2} \left(1 + \frac{\mathbf{p}_\mu^2}{3E_\mu^2}\right)\right], \quad (29c)$$

where  $\mathbf{p}_\mu$  is the muon 3-momentum and numerically  $|\mathbf{p}| = 29.79\text{MeV}$ , also  $E_{\nu\text{max}} = \frac{1}{2}E_\mu$ .  $\phi_0$  is a normalization factor which depends on factors such as number of protons on target and the number of pions produced per incident proton. Specific to the COHERENT experiment  $\phi_0 = \frac{rN_{\text{POT}}}{4\pi L^2}$ . The number of protons on target  $N_{\text{POT}} = 1.76 \times 10^{23}$  and  $r = 0.08$  is the number of neutrinos per flavor produced for each proton on target and  $L = 19.3$  m is the distance between the source and the CsI detector. Also the number of target nuclei in in Eq.(27) is given by  $n_{\text{CsI}} = \frac{N_A M_{\text{det}}}{M_{\text{CsI}}}$  where  $N_A$  is the Avogadro number  $M_{\text{det}} = 14.6$  kg is the detector mass and  $M_{\text{CsI}} = 259.8$  is the molar mass of CsI. For the total signal, one multiplies Eq.(27) by the lifetime of the experiment. An acceptance factor which depends on  $T$  is omitted but can be easily included.

In order to get a set-up independent prediction, we can focus on the ratios of the signal with  $\chi$  to the expected SM one. We first focus on the Z-mediated  $\text{CE}\nu\text{NS}$ . For our model, the total differential rate consists of the ones from SM neutrinos and those from  $\chi_\pm$ ,

$$\begin{aligned} \frac{dN_\chi}{dT} &= \frac{dN_{SM}}{dT} \times (1 - |U_4|^2 - |U_5|^2) + |U_4|^2 \frac{dN^{(Z)}(M_1)}{dT} + |U_5|^2 \frac{dN^{(Z)}(M_2)}{dT} \\ &= \frac{dN_{SM}}{dT} + |U_4|^2 \left(\frac{dN^{(Z)}(M_1)}{dT} - \frac{dN_{SM}}{dT}\right) + |U_5|^2 \left(\frac{dN^{(Z)}(M_2)}{dT} - \frac{dN_{SM}}{dT}\right) \end{aligned} \quad (30)$$

For notational simplicity we have dropped the flavor content of the incoming neutrino in the mixing elements, the other notation is obvious. Therefore, the ratio of total differential rate to the SM one deviates from unit by an amount of

$$1 - \frac{\frac{dN_\chi}{dT}}{\frac{dN_{SM}}{dT}} = |U_4|^2 \left(1 - \frac{dN^{(Z)}(M_1)}{dT} \Big/ \frac{dN^{(Z)}(0)}{dT}\right) + |U_5|^2 \left(1 - \frac{dN^{(Z)}(M_2)}{dT} \Big/ \frac{dN^{(Z)}(0)}{dT}\right), \quad (31)$$

note that  $\frac{dN_{SM}}{dT} = \frac{dN^{(Z)}(0)}{dT}$ . For simplicity, we assume  $|U_4|^2 = |U_5|^2 = |U_\chi|^2$ . Then, at a given

$T$ ,

$$\left(1 - \frac{dN_\chi}{dT} \bigg/ \frac{dN_{SM}}{dT}\right) |U_\chi|^{-2} = \left[2 - \frac{dN^{(Z)}(M_1)}{dT} \bigg/ \frac{dN^{(Z)}(0)}{dT} - \frac{dN^{(Z)}(M_2)}{dT} \bigg/ \frac{dN^{(Z)}(0)}{dT}\right], \quad (32)$$

which is displayed in Fig.4(a,c) for SNS<sup>2</sup> and nuclear power plant neutrino sources. The reactor neutrino flux in [22] is adopted. However, note that there is no SM counter part for the scalar-mediated coherent scattering, and the mixings are different from the Z-mediated ones. Therefore, the scalar-mediated part is separated and compared to the Z-mediated SM one,

$$\left(\frac{dN_H}{dT} \bigg/ \frac{dN_{SM}}{dT}\right) |U_H|^{-2} = \left[\frac{dN^{(H)}(M_1)}{dT} \bigg/ \frac{dN^{(Z)}(0)}{dT} + \frac{dN^{(H)}(M_2)}{dT} \bigg/ \frac{dN^{(Z)}(0)}{dT}\right]. \quad (33)$$

Again, we assume the couplings of the two shadow fermions are the same, and the quantity  $|U_H|^2$  is defined as

$$|U_H|^2 \equiv \frac{y_\chi^2 g_{HNN}^2}{M_H^2 G_F^2 Q_W^2} P_\chi^2 \simeq 0.7 \left(\frac{A}{N}\right)^2 y_\chi^2 P_\chi^2, \quad (34)$$

where

$$P_\chi = c_\alpha + s_\alpha \frac{v}{v_s} \frac{M_H^2}{M_\phi^2} \quad (35)$$

is of order unit as long as  $s_\alpha \lesssim 10^{-3}$ . If taking  $P_\chi^2 \sim 1$ , then  $|U_H|^2 \sim y_\chi^2$ . These are displayed in Fig.4(b,d). On the other hand, if  $s_\alpha > 10^{-3}$ , the process will be dominated by the light  $\phi$  and  $P_\chi^2 \gg 1$ .

Note that the scalar-mediated CE $\nu$ NS is not very sensitive to  $M_{1,2}$ . Also, observe the jumps at around  $T \sim 13\text{keV}$  in the SNS CE $\nu$ NS. They are due to sharp  $T_{max}$  cutoff from the monochromatic muon neutrino line, Eq.(29a).

It is seen that spallation neutron experiments are more sensitive to large splittings. Splitting of a 7keV and a 100keV will demand a very accurate measurement. This is to compare with reactor neutrino experiments which are less demanding in the signal but require a very low threshold for recoil energy, i.e.,  $T < 1\text{keV}$ . This is beyond current capabilities for most proposed experiments. Successful development of cryogenic detectors such as the proposed [23] experiment may bring these measurements to reality. As compare to Kurie plot experiments, neutrino-nucleus coherent scatterings cannot probe  $\chi$  splittings less than 100keV in the foreseeable future. On the positive side, they are sensitive to low energy scalar that can

---

<sup>2</sup> We have included the acceptance function of COHERENT experiment[21] for the estimation.



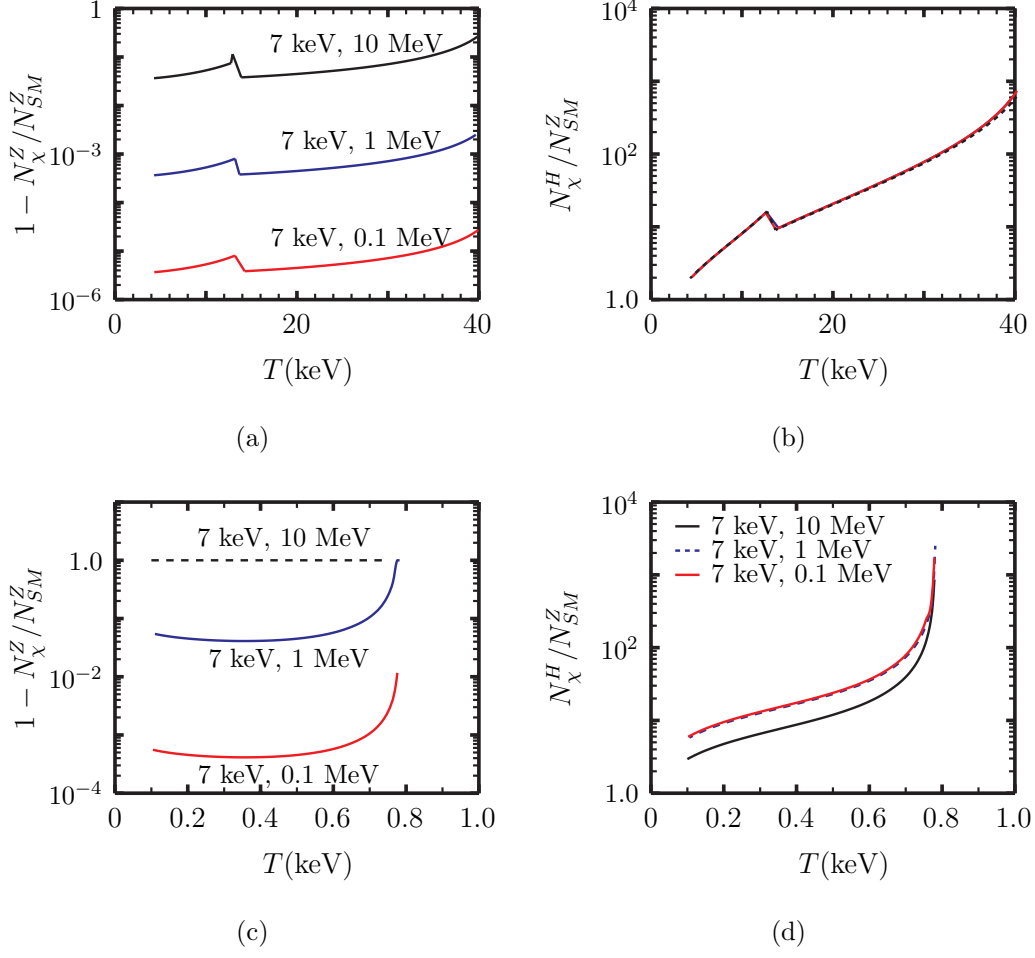


FIG. 4: (a) The deviation from the SM CE $\nu$ NS at the SNS neutrino source from  $Z$ -mediated scattering on the CsI target. (b) Same as (a) but mediated by scalar exchange. The deviations are in the unit of  $|U_\chi|^2$  and  $|U_H|^2$  for sub-diagram (a) and (b), respectively. Or equivalently, we set  $|U_\chi|^2 = 1$  and  $|U_H|^2 = 1$ .

(c) and (d): same as (a) and (b) with a nuclear power plant neutrino source.

mix with the Higgs boson. These fields are popular in Higgs portal constructions but are notoriously difficult to get an experimental handle on.

## V. ELECTROWEAK PRECISION TESTS

### A. Effects of kinetic mixing of $U(1)_Y$ and $U(1)_s$ .

The second portal of  $X_\mu$  can be studied independently of the other two portals. Firstly we note that the kinetic terms including the mixing can be recast into canonical form through

a  $GL(2)$  transformation. Explicitly, this is given by

$$\begin{pmatrix} X \\ B \end{pmatrix} = \begin{pmatrix} c_\epsilon & 0 \\ -s_\epsilon & 1 \end{pmatrix} \begin{pmatrix} X' \\ B' \end{pmatrix}, \quad (36)$$

where

$$s_\epsilon = \frac{\epsilon}{\sqrt{1-\epsilon^2}}, \quad c_\epsilon = \frac{1}{\sqrt{1-\epsilon^2}}. \quad (37)$$

After spontaneous symmetry breaking (SSB)  $X'$  and  $B'$  will mix, resulting in a shift in the SM  $Z$  mass. The physical neutral bosons consist of three states  $\gamma, Z, Z_s$ . The transformation relating the weak and mass basis is given by

$$\begin{pmatrix} B' \\ A_3 \\ X' \end{pmatrix} = \begin{pmatrix} c_W & -s_W & 0 \\ s_W & c_W & 0 \\ 0 & 0 & 1 \end{pmatrix} \begin{pmatrix} 1 & 0 & 0 \\ 0 & c_\eta & -s_\eta \\ 0 & s_\eta & c_\eta \end{pmatrix} \begin{pmatrix} \gamma \\ Z \\ Z_s \end{pmatrix}, \quad (38)$$

where  $s_W$  ( $c_W$ ) denotes  $\sin \theta_W$  ( $\cos \theta_W$ ) and similarly for the rotation angle  $\eta$ . The first rotation is the standard one that gives rise to the SM  $Z$  and the second one diagonalizes the mixing of the two  $Z$  bosons. The mixing angle is given by

$$\tan 2\eta = \frac{2s_W s_\epsilon}{c_W^2 (M_3/M_W)^2 + s_W^2 s_\epsilon^2 - 1}, \quad (39)$$

where  $M_3 \equiv g_s v_s$ ,  $\langle \phi \rangle = \frac{v_s}{\sqrt{2}}$ . We shall use the shorthand notation  $c_\eta(s_\eta) = \cos \eta(\sin \eta)$  and  $t_{2\eta} = \tan 2\eta$ . In general  $\epsilon$  is a free parameter; however, the success of the SM indicates that it has to be small. Clearly, the photon will remain massless, and the  $W$  bosons will be unchanged from the SM. Our notations follow that of [1] where details can be found.

The masses for the two massive neutral gauge bosons are readily found to be [1]

$$\begin{aligned} M_Z^2 &= M_Z^{2\text{SM}} \{c_\eta^2 - s_{2\eta} s_W s_\epsilon + s_\eta^2 s_W^2 s_\epsilon^2\} + s_\eta^2 M_3^2 \\ M_{Z_s}^2 &= M_Z^{2\text{SM}} \{s_\eta^2 + s_{2\eta} s_W s_\epsilon + c_\eta^2 s_W^2 s_\epsilon^2\} + c_\eta^2 M_3^2. \end{aligned} \quad (40)$$

We see that the  $Z$ -boson has its mass shifted from the SM value of  $M_Z^{\text{SM}} = \frac{M_W}{c_W}$  and receives a small contribution from the hidden sector. Similarly, the physical  $Z_s$  mass comes mainly from the hidden sector with a small contribution from the visible sector. We shall see later that if we want  $\chi$  to be warm dark matter, it is more natural to have  $M_{Z_s} \gg M_W$ . With that in mind then Eqs.(39,40) becomes

$$\eta \sim \frac{s_W s_\epsilon}{c_W^2} \frac{M_W^2}{M_3^2} \lesssim s_\epsilon \quad (41)$$

$$M_Z^2 \sim \left( \frac{M_W}{c_W} \right)^2 \left( 1 - \frac{s_W^2 s_\epsilon^2}{c_W^2} \frac{M_W^2}{M_3^2} \right). \quad (42)$$

The very precise measurement of the  $\rho$  parameter gives a stringent limit on the mixing parameters. The shift  $\delta\rho$  is

$$\delta\rho = \frac{s_W^2 s_\epsilon^2 M_W^2}{c_W^2 M_3^2} < 3.7 \times 10^{-4}.$$

In turn, we get

$$M_3 > 2.29 |s_\epsilon| \text{TeV}. \quad (43)$$

There are many electroweak precision tests (EWPT) that can set limits on  $\epsilon, \eta$ . In particular, the measurements at the Z-pole are independent on the mass of  $Z_s$  but are sensitive to the modifications to the SM fermion-fermion-Z couplings. These couplings are flavor universal and explicitly given by

$$Z^\mu \bar{f} f : i\gamma^\mu \frac{g_2}{c_W} \left[ (c_\eta g_f^L - s_\eta s_W s_\epsilon Y_f^L) \hat{L} + (c_\eta g_f^R - s_\eta s_W s_\epsilon Y_f^R) \hat{R} \right], \quad (44)$$

$$Z_s^\mu \bar{f} f : i\gamma^\mu \frac{g_2}{c_W} \left[ (-s_\eta g_f^L - c_\eta s_W s_\epsilon Y_f^L) \hat{L} + (-s_\eta g_f^R - c_\eta s_W s_\epsilon Y_f^R) \hat{R} \right], \quad (45)$$

where  $g_{L,R}^f = T^3(f_{L,R}) - s_W^2 Q^f$  is the coupling of the SM  $Z$  to fermions and  $\hat{L} = \frac{1-\gamma_5}{2}, \hat{R} = \frac{1+\gamma_5}{2}$ .

A comprehensive list of couplings used to constrain  $\epsilon$  can be found in [1].

## B. Invisible $Z$ decays

The two  $U(1)$ 's mixing will also modify the SM  $Z$  boson invisible decay width  $\Gamma_{\text{inv}}$ . There are two changes :(i) the modification of the  $Z - \nu - \nu$  couplings as given in Eq.(44), and (ii) the opening of the new channel  $Z \rightarrow \overline{\chi_{L,R}^c} \chi_{L,R}$  from the mixing with  $Z_s$ . The new invisible width is

$$\Gamma(Z \rightarrow \chi\chi) = \frac{c_\epsilon^2 s_\eta^2 g_s^2}{12\pi} M_Z, \quad (46)$$

where we have neglected the masses of  $\chi$ . The experimental value of  $\Gamma_{\text{inv}} = 499 \pm 1.5 \text{MeV}$  agrees well with 3 nearly massless active neutrinos. Thus

$$s_\eta^2 \left[ \frac{c_\epsilon^2 g_s^2}{3} - \frac{g_2^2}{8c_W^2} \right] \leq 2.1 \times 10^{-4}. \quad (47)$$

Other precision measurements constraints such as muon  $g - 2$ , atomic parity violation, and Møller Scattering are given in [1] and will not be repeated here.

### C. $Z \rightarrow f\bar{f}\phi$ decays

As will be discussed in the next section, in order for  $\chi$  to be WDM  $\phi$  is expected to be light,  $m_\phi \sim$  a few GeV, and long-lived,  $\tau_\phi \sim 1$  sec. Through the Higgs portal, the SM Z boson now can have a tree-level 3-body decays  $Z \rightarrow Z^*\phi \rightarrow \bar{f}f\phi$ , where  $f$  is the SM fermions. The decay branching ratio is calculated to be [19, 24]:

$$Br(Z \rightarrow \phi f\bar{f}) = \kappa_s^2 \times \mathcal{F}(M_\phi/M_Z) \times Br(Z \rightarrow f\bar{f}) , \quad (48)$$

where  $\kappa_s$  is the mixing between  $\phi$  and  $H$ , and

$$\mathcal{F}(x) = \frac{G_F M_Z^2}{24\sqrt{2}\pi^2} \left[ \frac{3x(20 - 8x^2 + x^4)}{\sqrt{4 - x^2}} \cos^{-1} \left( \frac{x}{2}(3 - x^2) \right) - 3(4 - 6x^2 + x^4) \ln x - \frac{1}{2}(1 - x^2)(47 - 13x^2 + 2x^4) \right] . \quad (49)$$

Due to its long lifetime,  $\phi$  will escape the detector, and the apparent signal will be  $Z \rightarrow \bar{f}f + \cancel{E}$ . The SM background will be  $Z \rightarrow \bar{f}f\bar{\nu}\nu$ . And  $f = \mu, b$  are ideal options to search for such processes and prob the scalar mixing squared,  $\kappa_s^2$ , down to  $10^{-7} - 10^{-8}$  with  $10^{12}$  fiducial Z's [24]. The smallest  $\kappa_s$  can be reached is still roughly one order too big for  $\phi$  to dilute the DM relic density. However, this search provides an interesting experimental cross check whether this model can accommodate the WDM in the way described in the next section.

## VI. $\chi$ AS WARM DARK MATTER

The previous discussions are independent of whether and how  $\chi$  can become WDM. Here we will examine the parameter space that allows  $\chi$  to be such. We intend to give a broad brush description of a possible scenario, and will leave many interesting details for a future study. Most of the discussions given below do not depend on the fact that physical  $\chi_\pm$  are Majorana fermions. If the splitting is small, then they will behave as one Dirac particle. If the splitting is large, then only the lighter one  $\chi_-$  will serve as DM. For clarity, we take  $\chi$  to be Dirac. The Majorana case can be obtained by  $\bar{\chi} \rightarrow \chi^c$  and use chiral projections where

needed. We will specifically explore the hierarchy of scale  $M_{Z_s} \gtrsim M_Z \gg M_\phi > M_\chi$ . The small  $Z_s - Z$  mixing will be denoted by  $\eta$ , see Eq.(39). After SSB of  $U(1)_s$ , the physical degrees of freedom in the hidden sector are  $Z_s, \chi, \phi^0$ , where  $\phi^0$  is the physical scalar  $\Re\phi$ . We shall also use the benchmark point  $M_\chi = 10\text{keV}, M_\phi = 2\text{GeV}$  to focus our discussion.

The secluded sector and the SM have very weak interactions through the portal interactions which are expected to be small. If the portal connections are switched off the two sectors will not establish thermal equilibrium, and cosmologically they evolve separately. If the portal interactions are small but not negligible, then the SM and the hidden sector can interact. In particular,  $\chi$  can interact with the SM fields via  $Z_s - Z$  mixing. The process  $\chi\bar{\chi} \leftrightarrow f\bar{f}$  where  $f$  is a SM fermion can proceed via such a mixing. The cross-section at temperature  $T$  can easily be estimated to be given by

$$\sigma v \sim \left( \frac{\eta g_s}{g_2} \right)^2 G_F^2 T^2 \equiv A_\chi^2 G_F^2 T^2, \quad (50)$$

where  $g_2$  is the SM  $SU(2)_L$  gauge coupling. If this rate falls below the Hubble expansion rate,  $\chi$  will freeze out. The freeze-out temperature  $T_f$  can be estimated by setting  $n\langle\sigma v\rangle$  to be equal to the Hubble expansion rate and  $n$  is the number density of the freeze-out particle. Thus,

$$\frac{3\zeta(3)}{2\pi^2} A_\chi^2 G_F^2 T_f^5 = \left( \frac{8\pi^3}{90} \right)^{\frac{1}{2}} \frac{T_f^2}{M_{pl}} \sqrt{g_*} \quad (51)$$

with  $g_*$  being the effective number of degrees of freedom. It is given by

$$g_* = \sum_{\text{bosons}} g_i + \frac{7}{8} \sum_{\text{fermions}} g_i \quad (52)$$

and  $g_i$  is the number of spin states.

From Eq.(51), the freeze-out temperature of  $\chi$  is controlled by the parameter  $A_\chi$ . From the electroweak constraints, Eq.(47),  $\eta g_s \lesssim \mathcal{O}(10^{-2})$ . Hence, it is natural to take  $A_\chi = .01$ , and we get

$$T_f = 40.6(g_*)^{\frac{1}{6}} \left( \frac{10^{-2}}{A_\chi} \right)^{\frac{2}{3}} \text{MeV}. \quad (53)$$

For a keV  $\chi$  which we are interested in, it is relativistic at the freeze-out. Such a situation will lead to over closure of the universe.

To see this, we note that the number density per entropy is

$$Y \equiv \frac{n_\chi}{s} \simeq \frac{135\zeta(3)}{4\pi^4 g_*(T_f)}. \quad (54)$$

$Y$  is thermally conserved and gives the relic density of  $\chi$  as

$$\Omega_\chi = \frac{Y m_\chi s}{\rho_c} \simeq 250 \times \left( \frac{m_\chi}{\text{keV}} \right) \left( \frac{1}{g_*(T_f)} \right). \quad (55)$$

where we have used the present day entropy density  $s = 2891.2 \text{cm}^{-3}$ , critical density  $\rho_c = 1.05371 \times 10^{-5} h^2 \text{GeVcm}^{-3}$  and  $h = 0.678$ [25]. This compares with the observed dark matter relic abundance[25] of

$$\Omega_{\text{DM}} = 0.258 \pm 0.011, \quad (56)$$

the estimate of Eq.(55) clearly over closes the universe unless  $g_*$  is of order 1000. In our model the  $g_*(T_f) \sim 31$  since it is below 1 GeV. Hence, some mechanism is required to bring down the value of  $\Omega_\chi$ . Moreover, Eq.(55) shows that the higher  $T_f$  is the less severe the over-closure problem is since  $g_*$  will be larger.

One way to get around this obstacle is to dilute the entropy. This can come from the decay of the scalar  $\phi^0$  if it has a long enough lifetime and decays into SM particles during the era  $\chi$  is freezing out. Note that  $\phi\phi$  cannot annihilate into SM fermions via  $Z_s - Z$  mixing. However, it can do so via mixing with the Higgs boson. It must be relativistic when  $\chi$  freezes out at  $T_f$  so that it has no Boltzmann suppression at decay. This should be earlier than  $T_f$  given in Eq.(51). This can be estimated as follows. The  $\phi^0\phi^0 H$  coupling is  $\sim \kappa v$  and gives

$$\sigma(\phi^0\phi^0 \rightarrow \bar{\mu}\mu) \simeq \left( \frac{\kappa v}{M_H^2} \frac{m_\mu}{M_W} \right)^2. \quad (57)$$

The freeze-out takes place when temperature yields  $n\sigma \lesssim \frac{T^2}{M_{pl}}$ , or

$$T \sim \kappa^{-2} \times 10^{-9} \text{GeV}. \quad (58)$$

With  $\kappa < 10^{-5}$ , it is ensured that  $\phi^0$  decouples relativistically and before  $\chi$  freezes out.

As  $\phi^0$  is unstable and can decay into SM fermions via mixing with Higgs, it will transfer the energy density into radiation while doing so. Using the sudden decay approximation that all the  $\phi$ 's decay at  $t \simeq \tau_\phi$  and reheat the universe to a temperature of  $T_r$ [26],

$$T_r \simeq 0.78 g_*(T_r)^{-\frac{1}{4}} \sqrt{\Gamma M_{pl}} = 1.11 \text{MeV} \left( \frac{1 \text{sec}}{\tau_\phi} \right)^{\frac{1}{2}}. \quad (59)$$

Where we have used  $g_* = 10.75$  and taken  $\phi$  lifetime to be  $\sim 1$  sec. The reason for taking this value is the constrain impose by BBN. In order not to upset a successful BBN,  $T_r$  should be larger than one MeV and this sets  $\tau_\phi \lesssim \mathcal{O}(1)$  second. Next we use energy conservation

$$m_\chi Y s(T_f) = \rho(T_r) = \frac{3}{4} s(T_r) T_r \quad (60)$$

and obtain the dilution factor

$$D \sim \frac{s(T_r)}{s(T_f)} = 280.4 \times \frac{g_*(T_r)^{\frac{1}{4}}}{g_*(T_f)} \left( \frac{m_\phi}{1\text{GeV}} \right) \left( \frac{1\text{sec}}{\tau_\phi} \right)^{\frac{1}{2}}. \quad (61)$$

Insertin this dilution factor into Eq.(55)the relic density of  $\chi$  is

$$\overline{\Omega_\chi} = \frac{0.89}{g_*(T_r)^{\frac{1}{4}}} \left( \frac{1\text{GeV}}{m_\phi} \right) \left( \frac{\tau_\phi}{1\text{sec.}} \right)^{\frac{1}{2}}. \quad (62)$$

Interestingly the dependence on  $g_*(T_f)$  cancels out with this entropy dilution mechanism. If we take  $T_r$  to be slightly higher than 1 MeV then Eq.(52) gives  $g_*(T_r) = 15.25$ , and with  $m_\phi = 2\text{GeV}$  one obtains the right amount of entropy dilution.

$\phi$  can decay into SM particles via the mixing with the SM Higgs. Its lifetime will depend on  $\kappa$  in Eq.(1) as well as other parameters in the scalar potential. The details are not important here and we will just denote this mixing by  $\kappa_s$ . The width of  $\phi \rightarrow f\bar{f}$  where  $f$  is a SM fermion is given by

$$\Gamma = \kappa_s^2 \frac{N_c \alpha m_f^2}{8M_W^2} m_\phi \beta_f^3, \quad (63)$$

where  $N_c$  is the color of  $f$ ,  $\beta_f = \sqrt{1 - 4m_f^2/m_\phi^2}$ , and  $\alpha$  is the fine structure constant. However, for  $m_\phi \simeq 2\text{GeV}$ , the main decay is into a gluon pair. The rate is estimated to be[19]

$$\Gamma_{gg} = \left( \frac{\alpha_s}{3\pi} \right)^2 \frac{m_\phi^2}{m_\mu^2} \frac{[6 - 2\beta_\pi^3 - \beta_K^3]^2}{\beta_\mu^3} \Gamma_{\mu^+\mu^-}. \quad (64)$$

Demanding that  $\tau_\phi \simeq 1$  sec. leads to

$$10^{-5} \gtrsim \kappa_s \gtrsim 1.3 \times 10^{-9}, \quad (65)$$

whereas the upper bound comes from previous considerations.

While we have identified the parameter space for  $\chi$  to be a WMD, we still have to ensure that there are no large processes that can generate significant numbers of  $\chi$  during or after thermal freeze-out. One process in which  $\chi$ 's can be produced is  $\phi^0\phi^0 \rightarrow \chi\bar{\chi}$ . This is suppressed by large seesaw mass  $M_N$  and can be neglected. Another source will be  $\phi^0 \rightarrow \chi\bar{\chi}$ . The effective coupling is given by  $y_{eff}^\chi \equiv \frac{f^2 v_s}{M_N}$ . We will require this mode to be less than the SM leads to a loose bound

$$y_{eff}^\chi < \kappa_s \frac{m_\mu}{M_W}. \quad (66)$$

A third process of producing  $\chi$  is via active  $\nu$  and  $\chi$  oscillations [27, 28]. This deserves a detailed study which is beyond our scope. We note that if this mechanism saturates the

bound on dark matter relic density, it gives a bound  $|U_{i\chi}|^2 \sim 10^{-9}(10\text{keV}/M_\chi)$  [9]. However, the entropy dilution mechanism will loosen the above constraint.

To conclude this section, we note that  $\phi$  in the mass range of  $1 - 10\text{GeV}$  is notoriously challenging for experiments to discover. A direct detection will be impossible at the LHC [29]. However, the Higgs boson invisible decay can be searched for via  $H \rightarrow \phi\phi$  and the pair of  $\phi$ 's will act as missing energy as noted before. The width is

$$\Gamma(H \rightarrow 2\phi) = \frac{\kappa_s^2 v^2}{32\pi M_H} \sqrt{1 - \frac{4M_\phi^2}{M_H^2}}. \quad (67)$$

The ATLAS[30] and CMS [31] place a limit on invisible branching ratio  $\mathcal{B}_{H \rightarrow inv} \lesssim 24 - 30\%$  at 95%C.L., which gives the constrain  $\kappa_s \lesssim .02$ . Hence, rare Z decays will still be the best probe of light and long-lived scalars.

## VII. CONCLUSIONS

We have explored a simple model of secluded sector consists of only a Dirac fermion  $\chi$  charged under a  $U(1)_s$ . It has vector couplings to  $U(1)_s$  and hence is not anomalous. Furthermore, it can acquire a bare mass term  $M_\chi \bar{\chi}\chi$ . Although  $M_\chi$  is a free parameter, it is of particular interest if it has a value  $\lesssim 1\text{MeV}$  that will make it a candidate for warm dark matter.

The secluded sector can be connected to the SM via three kinds of portals. The first is the seesaw portal (SP). It consists of three SM singlet righthanded neutrinos  $N_R$ 's which allows us to implement type-I seesaw for active neutrino masses. The second portal is due to the kinetic mixing of  $U(1)_s$  and the SM hypercharge  $U(1)_Y$ . This is the gauge portal (GP).  $U(1)_s$  symmetry is broken spontaneously at a scale  $v_s$  below the seesaw scale by a SM singlet scalar  $\phi$ . We also take  $v_s > v$ . The gauge invariant term  $\phi^\dagger \phi H^\dagger H$  provides the third portal. This is commonly known as the Higgs portal (HP). Moreover, the gauge invariant  $\chi N_R \phi$  Yukawa couplings provide an indirect connection between  $\chi$ 's and the SM sector after  $N_R$  is integrated out. All three portals have been discussed independently as simplified models for dark matter. Taken all three together reveals features that are not present in the simplified 1-portal models.

SP not only provides the seesaw mechanism for active neutrinos, but it also splits  $\chi$  into two Majorana fermions. These can form Dirac mass terms with the active neutrinos. They



act very much like sterile neutrinos although they are not. They originate from the hidden sector. They add to the structure of the neutrino mass matrix and contribute to  $0\nu\beta\beta$  decays. They make their presence felt in the Kurie plots of  $\beta$  decays of nuclei as well as coherent low energy scattering of nuclei. The latter experiments have the added advantage that they can probe the new  $\nu - \chi - \phi^0$  vertex which  $\beta$  decay experiments do not.

In addition to producing a new gauge boson  $Z_s$ , the GP also allows  $\chi$  to interact with the SM. This allows  $\chi$  to be thermally produced dark matter candidate. The phenomenology of the  $Z_s$ , whose mass is expected to be in TeV, can be probed in electroweak precision measurements [1] and directly searched for at the LHC. The new invisible decay of the SM Z will also be an exciting channel for the Z-factory option of future lepton colliders such as the FCC-ee and CEPC[32, 33].

In this study, we also found a new role for the portal scalar  $\phi^0$ . If it has a mass in the GeV range, it can act as an agent for entropy dilution and bring the relic density of the thermally produced  $\chi$  to the range of the observed value. It can also be looked for in precision measurements of the Z-boson at the Z-factory[24].

Although the model we explored is self-contained and renormalizable, it suffers from the same hierarchy problem that plagues the SM because of the use of an elementary scalar. The  $U(1)_s$  symmetry also has a Landau pole problem as in QED. Hence, it is reasonable to assume that it should be embedded in a more elaborate dark sector. If that is the case, one needs not demand  $\chi$  to be a dark matter candidate. This opens up regions of parameter space that we have not discussed. We reiterate that the region of parameter space we have studied was motivated by looking at  $\chi$  as a WDM candidate. The search of signatures for  $\chi$ ,  $Z_s$  and  $\phi$  in experiments we have discussed should be conducted with this general setting in mind.

## Acknowledgments

WFC is supported by the Taiwan Ministry of Science and Technology under Grant No. 106-2112-M-007-009-MY3. TRIUMF receives federal funding via a contribution agreement with the National Research Council of Canada and the Natural Science and Engineering Research Council of Canada.

## Note Added

After the paper was completed, we were informed that similar considerations of new fermions production in coherent neutrino-nucleus scattering was done in [34]. We agree with their results where they overlap with ours. Ref [35] considered a similar set up with radiative neutrino mass generations.

- 
- [1] W. F. Chang, J. N. Ng and J. M. S. Wu, Phys. Rev. D **74**, 095005 (2006) Erratum: [Phys. Rev. D **79**, 039902 (2009)].
  - [2] W. F. Chang, J. N. Ng and J. M. S. Wu, Phys. Rev. D **75**, 115016 (2007).
  - [3] E.W. Kolb and M.S. Turner, The Early Universe , Perseus Press , (1990)
  - [4] J.S. Bullock and M. Boylan-Kolchin, Ann. Rev. Astron. Astrophys. **55** 343 (2017)
  - [5] J.F. Navarro, C.S. Frenk, and S.D.M. White Atsrophy. J. Lett. **490** 493 (1997)
  - [6] W.J.G. de Blok, Adv. Astron. **2010** 789293 (2010)
  - [7] E. Bulbul, *et.al.*, Astrophys. J. , **789** 13 (2014)
  - [8] A. Boyarski, O. Ruchayskiy, D. Iakubovskiy, and J. Franse, Phys. Rev. Lett. **113** 251301 (2014)
  - [9] A. Boyarski, M. Drewes, T. Lasserre, S. Mertens, and O. Ruchayskiy, Prog. Part. Nucl. Phys. **104** 1 (2019). arXiv: 1807.07938 [hep-ph]
  - [10] S. Weinberg, Phys. Rev. Lett. **43** 1566 (1979)
  - [11] T. Asaska, S. Blanchet, and M. Shaposhnikov, Phys. Lett. **B 631** 151 (2005)  
T. Asaska, and M. Shaposhnikov, Phys. Lett. bf B620 17 (2005)
  - [12] B. Pal and L. Wolfenstein, Phy. Rev. **D25** 766 (1982)
  - [13] G.C. McLaughlin and J.N. Ng, Phys. Rev. **D63** 053002 (2001)
  - [14] H.J. de Vega, O. Moreno, E. Moya de Guerra, M. Ramón Medrano, and N.G. Sáanchez, Nucl. Phys. **B866** 177 (2013).
  - [15] C. Weinheimer, arXiv:0912.1619 [hep-ex]
  - [16] S. Mertens, *et.al.*, TRISTAN project. arXiv 1810.06711 [physics-ins-det]
  - [17] D. Akimov et al., COHERENT collaboration, Science **357** 1123 (2017) [arXiv: 1708.01294]
  - [18] J.Billard et al. J.of Phys. G: Nucl. Part. Phys. **44** 105101 (2017)

- [19] J.F. Gunion, H.H. Haber, G. Kane and S. Dawson, The Higgs Hunter's Guide, Perseus Pub. (1990)
- [20] D.Z. Freedman, Phys. Rev. **D9** 1389 (1974)
- [21] D. Aristizabal Sierra, V. De Romeri and N. Rojas, Phys. Rev. D **98**, 075018 (2018).
- [22] H. T. Wong *et al.* [TEXONO Collaboration], Phys. Rev. D **75**, 012001 (2007).
- [23] R. Strauss *et al.*, Eur. Phys. J. **C77** 506 (2017)
- [24] W. F. Chang, J. N. Ng and G. White, Phys. Rev. D **97**, no. 11, 115015 (2018).
- [25] M. Tanabashi *et al.* [Particle Data Group], Phys. Rev. D **98**, no. 3, 030001 (2018).
- [26] R.J. Sherrer and M.S. Turner, Phys. Rev. **D31** 681 (1985)
- [27] S. Dodelson and L.M. Widrow, Phys. Rev. Lett. **72** 17 (1994)
- [28] A.D. Dolgov and S.H. Hansen, Astropart. Phys. **16** 339 (2002).
- [29] W. F. Chang, T. Modak and J. N. Ng, Phys. Rev. D **97**, no. 5, 055020 (2018).
- [30] G. Aad *et al.* (ATLAS Collaboration), J. High Energy Phys. 01 (2016) 172.
- [31] V. Khachatryan *et al.* [CMS Collaboration], JHEP **1702**, 135 (2017).
- [32] C.-S.S. Group, CEPC-SPPC Preliminary Conceptual Design Report. 1. Physics and Detector, <http://www.Inf.infn.it/sis/frascatiseries/Volume61/Volume61.pdf>
- [33] D. d'Enterria, Physics at the FCC-ee, in Proceedings of 17th Lomonosov Conference on Elementary Particle Physics. ( World Scientific, Moscow, Russia, 2017) p.182
- [34] V. Brdar, W. Rodejohann and X. J. Xu, JHEP **1812**, 024 (2018).
- [35] P. Ballett, M. Hostert and S. Pascoli, arXiv:1903.07589 [hep-ph], P. Ballett, M. Hostert and S. Pascoli, arXiv:1903.07590 [hep-ph].